

Assessing the utility of satellite-based whitecap fraction to estimate sea spray production and CO₂ transfer velocity

To the memory of Dr. Edgar L. Andreas

M D Anguelova

Remote Sensing Division, Naval Research Laboratory, Washington, DC, USA

maggie.anguelova@nrl.navy.mil

Abstract. The utility of a satellite-based whitecap database for estimates of surface sea spray production and bubble-mediated gas transfer on a global scale is presented. Existing formulations of sea spray production and bubble-mediated CO₂ transfer velocity involve whitecap fraction parametrization as a function of wind speed at 10 m reference height $W(U_{10})$ based on photographic measurements of whitecaps. Microwave radiometric measurements of whitecaps from satellites provide whitecap fraction data over the world oceans for all seasons. Parametrizations $W(U_{10})$ based on such radiometric data are thus applicable for a wide range of conditions and can account for influences secondary to the primary forcing factor, the wind speed. Radiometric satellite-based $W(U_{10})$ relationship was used as input to: (i) the Coupled Ocean-Atmosphere Response Experiment Gas transfer (COAREG) algorithm to obtain CO₂ transfer velocity and total CO₂ flux; and (ii) the sea spray source function (SSSF) recommended by Andreas in 2002 to obtain fluxes of sea spray number and mass. The outputs of COAREG and SSSF obtained with satellite-based $W(U_{10})$ are compared with respective outputs obtained with the nominal $W(U_{10})$ relationship based on photographic data. Good comparisons of the gas and sea spray fluxes with direct measurements and previous estimates imply that the satellite-based whitecap database can be useful to obtain surface fluxes of particles and gases in regions and conditions difficult to access and sample in situ. Satellite and in situ estimates of surface sea spray production and bubble-mediated gas transfer thus complement each other: accurate in situ observations can constrain radiometric whitecap fraction and mass flux estimates, while satellite observations can provide global coverage of whitecap fraction and mass flux estimates.

1. Introduction

Direct measurements of near-surface ocean processes under high winds remain problematic due to the difficulty of operating surface vessels and in situ instrumentation under gale conditions. Such measurements are necessary to better constrain parameterizations of near-surface ocean processes and improve predictions of weather and climate models. Whitecaps are the surface expression of various air-sea processes enhanced by wave breaking. Whitecap fraction W —defined as the fraction of the sea surface covered with sea foam—is thus a forcing variable suitable for parameterizing surface fluxes associated with breaking waves and whitecaps such as surface production of sea spray aerosol and bubble-mediated gas exchange across the air-sea interface. Whitecap fraction is usually obtained from photographs by applying an intensity threshold $W(I)$ to discriminate whitecaps from the surrounding water. Photographic $W(I)$ data have been used extensively to derive parameterizations of W as a function of wind speed at 10 m reference height $W(U_{10})$. Surface fluxes of particles and gases can be estimated



globally by combining a $W(U_{10})$ expression with global maps of U_{10} . However, available $W(U_{10})$ relationships do not capture the full variability of the oceanic whitecaps because many other factors beside U_{10} affect the formation and behavior of the bubbles comprising the whitecaps.

Experiments have shown strong correlation of whitecap fraction and gas transfer velocity with microwave brightness temperature T_B [1]. Observations of ocean surface T_B carry information about the whitecaps because T_B responds directly to the surface roughness and sea foam as they are affected by U_{10} , wave field history, and seawater properties (e.g., temperature, salinity, and presence of organic compounds) [2]. Attenuation of the electromagnetic radiation at microwave frequencies (e.g., 6–40 GHz) by atmospheric gases, water vapors, and clouds is well characterized and affords all-weather information on oceanic whitecaps from satellite-borne radiometers. Use of satellite-based whitecap fraction to parameterize gas exchange and other surface fluxes of mass and energy can thus alleviate the difficulties of direct in situ measurements of surface fluxes under high winds and potentially improve the flux accuracy by accounting for the whitecap variability caused by secondary factors.

An algorithm obtaining W from satellite observations, developed at the Naval Research Laboratory, combines T_B data from WindSat radiometer, a model for atmospheric attenuation at microwave frequencies, and physically-based models for the emissivity of rough sea surface and emissivity of foam [3]. The whitecap database built with this algorithm compiles $W(T_B)$ values for entire year 2006 matched in time and space with data for the wind vector (speed and direction), wave field (e.g., significant wave height and peak wave period), and environmental parameters (e.g., sea surface temperature and atmospheric stability) from different sources [4]. This database has proved useful in analyzing and quantifying the variability of W [5].

By their measuring principle, microwave radiometers provide the total whitecap fraction $W(T_B)$, including foam generated during active wave breaking and residual foam left behind by these breaking waves [6]. The total whitecap fraction W is important for estimating the sea spray aerosol production and heat exchange between the ocean and the atmosphere. However, the active portion W_A is necessary for evaluating turbulent processes such as mixing of the upper ocean, gas exchange, ocean ambient noise, and spray-mediated intensification of tropical storms [7]. Sensitivity of microwave frequency to foam thickness allows association of W_A with $W(T_B)$ at 10 GHz (hereafter referred to as W_{10}) and W with $W(T_B)$ at 37 GHz (referred to as W_{37}) [5, 6]. Because this is a crude separation of active and residual whitecaps, we have developed a scaling factor $R = W_A/W$, which, when applied to satellite-based data $W(T_B)$, can provide data for W_A on a global scale [8]. The procedure separating active and residual whitecaps uses the Philips concept for breaking crest length distribution [9] and energy dissipation rate ε [10].

Here, we present estimates of carbon dioxide (CO_2) transfer velocity and the sea spray production flux, and assess differences due to use of $W(U_{10})$ parameterizations based on photographic or radiometric W data. Use of W_A values instead of W and the applicability of satellite-based whitecap fraction values for estimating surface fluxes of particles and gases are discussed.

2. Methods

2.1. CO_2 transfer velocity and flux

A physically-based algorithm for bulk meteorological and gas transfer fluxes has been developed using data from the Coupled Ocean-Atmosphere Response Experiment (COARE) [11]. Consistently adding new observations from different field campaigns, the COARE working group has been steadily improving the representation of the meteorological and gas fluxes in the COARE algorithm [11]. Data from three Gas Exchange (GasEx) field campaigns have been used to implement the COARE gas transfer algorithm (designated COAREG) [12].

The COAREG algorithm has taken the representation of the gas transfer velocity k away from simple power laws in terms of U_{10} and currently partitions k into waterside and airside components [12]. Each component is formulated in terms of forcing variables (e.g., U_{10} or friction velocity u_*), gas solubility, and gas diffusivity (Schmidt number). The waterside term k_w includes molecular-turbulent (or direct) transfer and bubble-mediated transfer k_b . The bubble-driven term k_b is taken from Woolf [13] and

involves the wind speed parameterization of whitecap fraction $W(U_{10})$ among other variables. Two parameters, A and B , in k_w are used as tuning parameters, their values adjusted every time new gas flux observations (or process parameterizations) are available. Importantly, parameters A and B can be used to judge how well the physical formulations in the COAREG algorithm represent the modeled processes and forcing factors. Specifically, because COAREG represents the gas transfer physics on the basis of the similarity hypothesis, the empirical constants A and B should be the same for all gasses.

The latest version COAREG3.1 [12] has been used in this study with meteorological data from the Southern Ocean (SO) GasEx field campaign [14]. The whitecap fraction parameterization used in the bubble-mediated transfer velocity k_b is that developed by Monahan and O’Muircheartaigh [15] (hereafter referred to as MOM80):

$$W(U_{10}) = 3.84 \times 10^{-6} U_{10}^{3.41} \quad (1)$$

COAREG3.1 uses $A = 1.6$ and $B = 1.8$, values adjusted to fit data from all three GasEx campaigns and wind stress representation with tangential and wave components [12]. Algorithm version COAREG3.1 produces a good fit to field observations using the same A and B values for two gases, CO_2 and DMS (dimethyl sulfide) (e.g., figure 4 in [12]). One aspect to be addressed in future COAREG versions is to reconcile predictions for the total transfer velocity (normalized to a fixed Schmidt number of 660) k_{660} from COAREG3.1 to eddy correlation (atmospheric) gas flux measurements during GasEx campaigns [14] and to the quadratic dependence $k_{660}(U_{10})$ based on dual tracer (oceanographic) gas flux measurements [16].

2.2. Sea spray production flux

Sea spray production flux is necessary for estimating sea spray aerosol loadings in the atmosphere and the spray-mediated heat fluxes. The number or mass of small sea spray aerosols (radii at formation $r_0 \leq 1.6 \mu\text{m}$) are needed when modeling the direct scattering of shortwave radiation and modifications of cloud properties by sea salt particles. Loadings of large sea spray aerosols ($r_0 > 1.6 \mu\text{m}$) are needed to evaluate the contribution of sea spray to enthalpy flux (the sum of sensible and latent heat fluxes) and its role for intensification of tropical storms. For chemical transport models, surface and volume provided by the sea spray particles are needed to assess heterogeneous chemical reactions occurring on or within sea spray droplets.

Sea spray production flux is quantified with a sea spray source function (SSSF), which predicts the rate at which sea spray droplets at a given size dF/dr_0 are produced at the sea surface. SSSF has two main dependencies: (i) size dependence, which gives the shape of the SSSF over the range of sea spray sizes; and (ii) wind speed dependence, which gives the magnitude of the flux. In this study, we use the SSSF recommended by [17]. In this SSSF, the wind speed dependence is introduced via MOM80 whitecap fraction given with (1). The size dependence is presented with the size distributions of Monahan *et al.* [18] for small ($0.8 \leq r_0 \leq 1.6 \mu\text{m}$) and Andreas [19] for large ($1.6 \leq r_0 \leq 500 \mu\text{m}$) droplets.

2.3. Whitecap fraction

There are whitecap fraction data available now from three different measuring methods (section 1), namely photographic data $W(I)$, radiometric data $W(T_B)$, and data from energy dissipation rate using a $W_A(\epsilon)$ expression. Figure 1 (solid line) shows the MOM80 parameterization $W(U_{10})$ given with (1). The available photographic data $W(I)$ (circles, [2, their table 2]) cluster around the MOM80 $W(U_{10})$ parameterization. Data for wind speed and wave spectra from buoy 41001 have been used to obtain ϵ and then calculate active whitecap fraction $W_A(\epsilon)$ (diamonds in figure 1). Values $W_A(\epsilon)$ compare reasonably well with photographic $W_A(I)$ data (crosses in figure 1). Satellite-based data $W(T_B)$ at frequencies of 10 and 37 GHz, matched in time and space with data from buoy 41001, are also shown in figure 1 (squares and triangles). Both photographic $W(I)$ and radiometric $W(T_B)$ data are one to two orders of magnitude larger than active whitecap fraction data $W_A(I)$ and $W_A(\epsilon)$. Overall, whichever

method of separating W and W_A is used, most values of active whitecap fraction lay below the MOM80 $W(U_{10})$ curve.

The question how best to use the satellite-based $W(T_B)$ data has been reasoned by Albert *et al.* [20]; i.e., should we use the data directly or should we use them to first derive a new $W(U_{10})$ parameterization. Using the $W(T_B)$ values directly limits the uncertainty to that of estimating $W(T_B)$ from satellite observations and does not add uncertainty from deriving an expression for $W(U_{10})$. Alternatively, a new $W(U_{10})$ parameterization can be used with readily available wind speed data. Importantly, such a parameterization will be globally applicable because the whitecap database from which it is derived covers the full range of meteorological conditions encountered over the world oceans for all seasons.

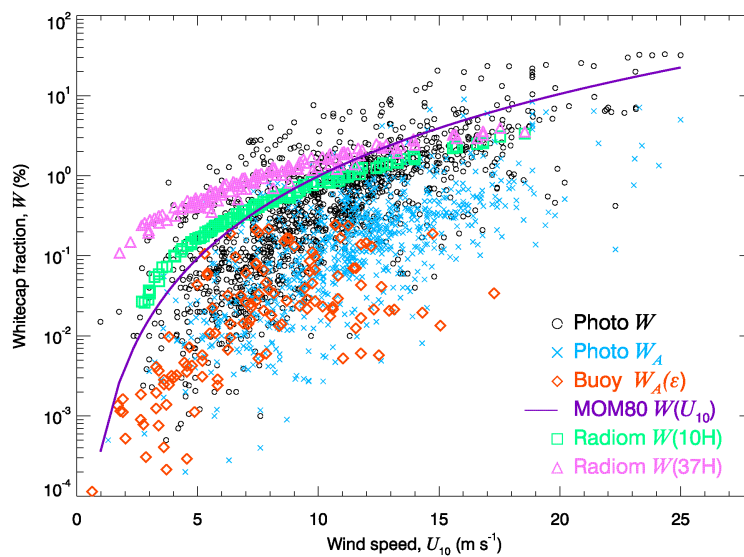


Figure 1. Whitecap fraction obtained with different methods as a function of wind speed at 10 m reference height U_{10} : total whitecap fraction W from photographs (circles); active whitecap fraction from photographs W_A (crosses); total whitecap fraction from satellite observations of brightness temperature at 10 and 37 GHz, horizontal (H) polarization (squares and triangles); active whitecap fraction from energy dissipation rate ϵ (diamonds); parameterization $W(U_{10})$ based on photographic W data (solid line).

The large number of W values from the whitecap database ensures low error in the derivations of the $W(U_{10})$ expression from satellite observations. In this study, we used the $W(U_{10})$ parameterizations based on $W(T_B)$ values for 10 and 37 GHz [5]:

$$W_{10} = 4.6 \times 10^{-3} \times U_{10}^{2.26}; \quad 2 < U_{10} \leq 20 \text{ m s}^{-1}, \quad (2a)$$

$$W_{37} = 3.97 \times 10^{-2} \times U_{10}^{1.59}; \quad 2 < U_{10} \leq 20 \text{ m s}^{-1}, \quad (2b)$$

Analysis of the $W(T_B)$ database implied that the influence imparted to secondary factors on whitecap fraction is likely well captured by quadratic wind speed dependence [20]. The wind exponents of 2.26 for W_{10} and 1.56 for W_{37} in (2) thus reflect the effects of additional factors well. Importantly, the deviations of the wind exponents in (2) from the quadratic exponent account for specifics pertinent to active and residual whitecaps, namely more wind and turbulence influence on W_{10} and more bubble property influence on W_{37} .

For this study, we have run COAREG3.1 and SSSF first with (1), the nominal choice for whitecap fraction $W(U_{10})$ in the respective formulations. We then ran COAREG3.1 and SSSF with (2) at all other parameters the same, i.e., changing only the $W(U_{10})$ relationship. Comparing the results from the two runs, we gain insights for the differences in CO_2 transfer velocity, CO_2 flux, and sea spray production due to using a whitecap fraction with different (or absent) representation of secondary influences. The difference for a variable x obtained once with the nominal (photographic) $W(U_{10})$ and then with the new (radiometric) $W(U_{10})$ relationships is quantified as percent change (PC) defined as:

$$PC = \Delta x/x = 100(x_{new} - x_{nominal})/x_{nominal} \quad (3).$$

3. Results and discussion

Figure 2 shows bubble-mediated transfer velocity k_b obtained with (1) and (2). For wind speeds ranging from 0.5 to $\sim 21 \text{ m s}^{-1}$, k_b values vary from $< 10^{-4}$ to $\sim 100 \text{ cm h}^{-1}$. The satellite-based values for k_b are larger than the nominal k_b values for wind speeds below $\sim 10 \text{ m s}^{-1}$ and smaller for high winds (above 15 m s^{-1}). This is caused by wind speed exponents lower in (2) than that of MOM80 in (1). There is little significance to the disagreement at low wind speeds, with $\Delta k_b/k_b \gg 200\%$ from (3), considering that the wind speed for the onset of whitecapping ranges from 3 to $\sim 6 \text{ m s}^{-1}$ [2, their table 1]. The k_b values obtained with (2a) at 10 GHz are closer to the nominal k_b values from COAREG3.1 than k_b values obtained with (2b) at 37 GHz. Because W_{10} from (2a) represents predominantly active whitecaps with only partial contribution from residual whitecaps (section 1), W_{10} is more suitable for gas exchange estimates than W_{37} . For $U_{10} > 10 \text{ m s}^{-1}$, the use of (2a) leads to underestimation of k_b compared to the nominal COAREG3.1 k_b by no more than 60%, i.e., from (3) $\Delta k_b/k_b = (-60, 0)\%$.

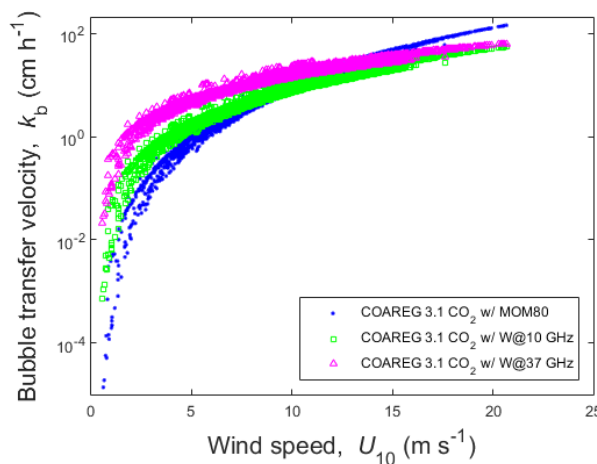


Figure 2. Bubble-mediated transfer velocity k_b as a function of wind speed U_{10} .

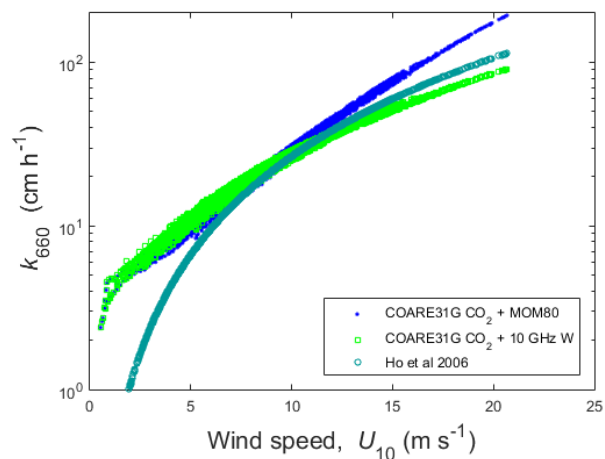


Figure 3. Normalized transfer velocity k_{660} as a function of wind speed U_{10} .

Figure 3 shows how the difference in k_b translates to a difference in the (normalized) total transfer velocity k_{660} (recall section 2.1). The satellite-based k_{660} values compare closely with the nominal COAREG3.1 k_{660} for wind speeds up to about 10 m s^{-1} . At higher winds, satellite-based k_{660} values are closer to the quadratic relationship obtained from dual tracer observations than to the COAREG3.1 values tuned to the eddy correlation observations (section 2.1). Comparison of time series of the total CO_2 flux F_{CO_2} (figure 4) shows that the use of (2a) instead of (1) yields differences $\Delta F_{\text{CO}_2}/F_{\text{CO}_2}$ from +13% to -53% (figure 5) with an average underestimation of $\sim -6\%$. The largest difference (around yearday 100) is for a period with the highest wind speed. As expected, the use of (2b) yields overestimation of the total CO_2 flux with $\Delta F_{\text{CO}_2}/F_{\text{CO}_2}$ of $\sim +30\%$ on average.

The estimates shown in figures 2–5 are obtained using the total whitecap fraction values $W(I)$ and $W(T_B)$. As the data shown in figure 1 suggest, if we use active whitecap fraction values $W_A(I)$ or $W_A(\epsilon)$ instead of W , we would obtain much lower bubble-mediated and total normalized CO_2 transfer velocity and flux, by at least a factor of 10. Such low estimates would be in stark contradiction with the COAREG values, which have been adjusted to direct measurements. This implies that, though W_A is considered

more suitable for gas exchange occurring during the turbulent phase of the wave breaking, some mix of upper limit values of W_A and lower limit values of W may represent the gas transfer well.

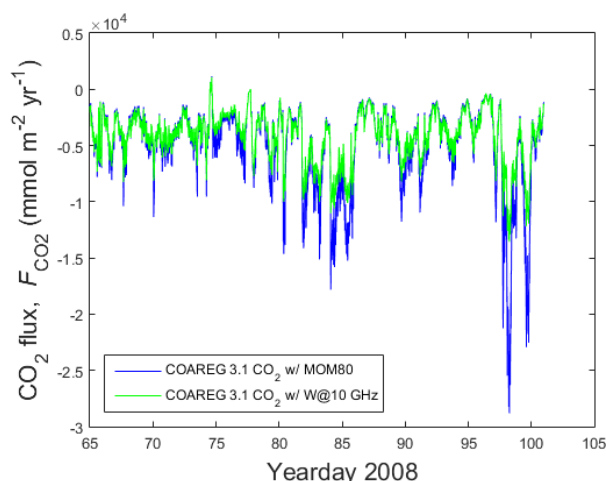


Figure 4. Time series of air-sea CO_2 flux.

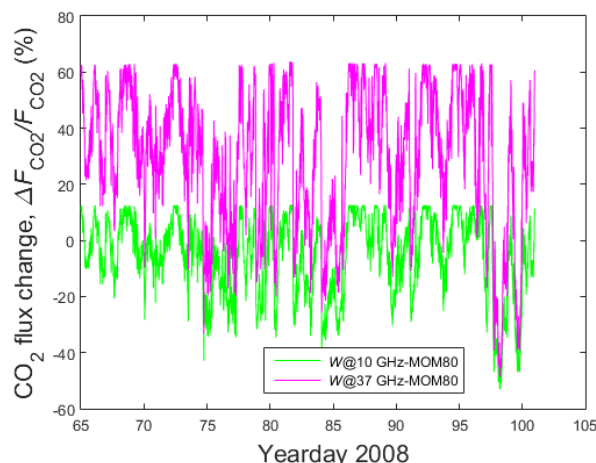


Figure 5. Time series of the percent change of air-sea CO_2 flux due to change of $W(U_{10})$ relationship.

Figure 6 shows the size-resolved sea spray number flux at wind speed 15 m s^{-1} . The vertical (dotted) line at $1.6 \mu\text{m}$ marks the portions of the size spectrum modeled as small and large particles (section 2.2). Using the same size distributions in SSSF but changing the $W(U_{10})$ relationship from (1) to (2), we obtain lower sea spray fluxes. The sea spray flux obtained with W_{10} (dashed line) is by a factor of 2 lower than the flux estimated with MOM80 parameterization (dash-dot line). This is an upper limit of the photographic versus radiometric differences because the flux dF/dr_0 at 37 GHz obtained with (2b) (solid line) has values between those of dF/dr_0 obtained with (1) and (2a). Considering that both active and residual whitecaps contribute to the bubble-mediated production of sea spray droplets, W_{37} is more suitable for estimates of spray-driven heat fluxes than W_{10} . Figure 7 shows a difference map of sea spray fluxes at $r_0 = 10 \mu\text{m}$ calculated with (1) and (2b) for one day (27 March 2006). According to the map, at this size, sea spray number flux dF/dr_0 obtained with (1) is higher (lower) at high (low) latitudes than dF/dr_0 obtained with (2b) by up to ± 300 particles.

The annual rate of total (size integrated) sea spray mass flux dF for March 2006 is shown in figure 8. From such maps, we estimated global mean of sea spray production of 5.64 Pg yr^{-1} . This estimate is comparable to the values of Jaeglé *et al.* [21] and Sofiev *et al.* [22] (4.86 and 5.87 Pg yr^{-1} , respectively), and it differs by less than a factor of 2 from the values reported by Norris *et al.* [23] and Grythe *et al.* [24] (3.25 and 8.91 Pg yr^{-1} , respectively). While the differences can be partially explained with flux integration over different sizes in different studies, it is noteworthy that these previous estimates are based either on direct observations (e.g., Norris *et al.* [23] uses direct eddy correlation measurements) or on SSSFs modified to better account for additional factors (e.g., SST in Jaeglé *et al.* [21]).

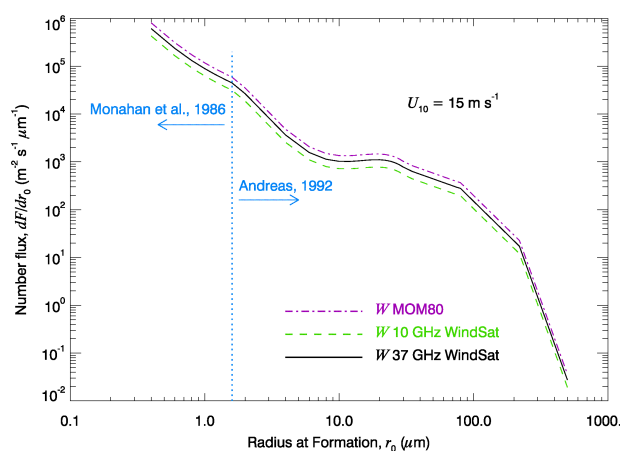


Figure 6. Size-resolved sea spray number flux at wind speed 15 m s^{-1} obtained with different formulations of the whitecap fraction wind speed dependence $W(U_{10})$. The vertical line marks small and large sea spray radii at formation r_0 calculated with different size distributions.

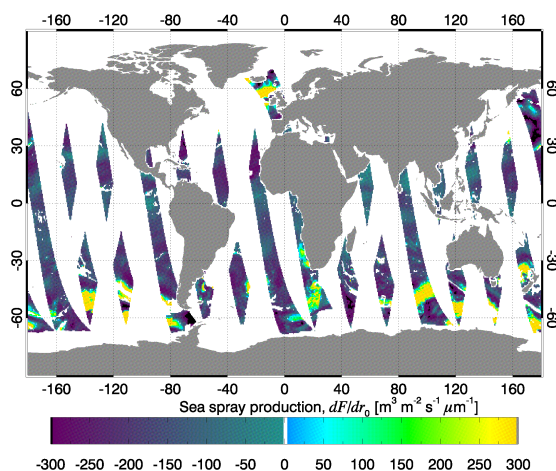


Figure 7. Daily map for 27 March 2006 (grid cells of $0.5^\circ \cdot 0.5^\circ$) of the difference of sea spray number fluxes at $r_0 = 10 \text{ μm}$ obtained with $W(U_{10})$ of MOM80 and WindSat: positive anomalies (light colors) show that $dF/dr_0(\text{MOM80}) > dF/dr_0(\text{WindSat})$.

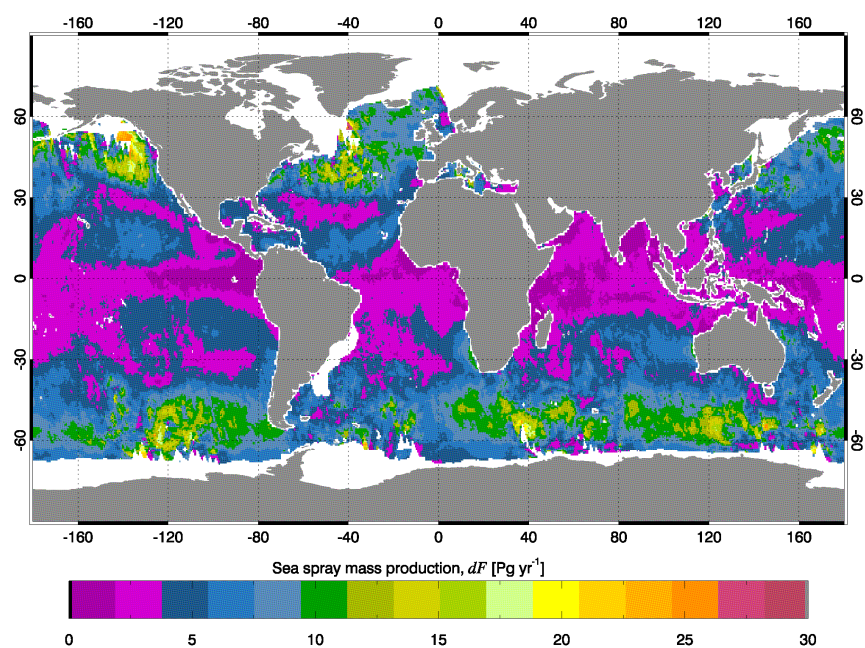


Figure 8. Monthly map (March 2006) of annual rate of total (integrated by size) sea spray mass production obtained with satellite-based estimates of whitecap fraction at frequency 37 GHz (equation 2b).

4. Summary

Surface fluxes of CO_2 and sea spray production have been calculated using satellite-based data for whitecap fraction. The calculated values compare reasonably well with previous estimates of CO_2 transfer velocity (within 10%–60%) and sea spray mass flux (differences less than a factor of 2). Use of active whitecap fraction values would predict CO_2 transfer velocity and flux too low (approximately an order of magnitude) compared to direct observations. The results thus suggest that the upper limit of W_A

data combined with the lower limit W data would provide whitecap fraction and bubble-mediated CO_2 transfer values that would reproduce the gas exchange characteristics observed with the in situ measurements. For sea spray production flux, satellite-based whitecap fraction at both 10 and 37 GHz produce fair comparisons with previous estimates. A notable implication of these results is the possibility to use satellite-based radiometric measurements of whitecap fraction to obtain surface sea spray production and bubble-mediated gas transfer on a global scale.

Acknowledgments

This paper is dedicated to the memory of Ed Andreas, a long-admired colleague, mentor (as a member of my PhD committee), and friend. Ed's deep knowledge of physical oceanography and boundary layer turbulence, innovative research on sea spray production, vast field experience in the Arctic and Antarctic, and mastery of technical writing have shaped my work and career for years. In friendly conversations and regular correspondence, Ed was invariably inspiring and generous with his advice, trust, and encouragement. He is greatly missed.

References

- [1] Wang Q *et al* 1995 *Air-Water Gas Transfer* ed B Jähne and E C Monahan (Hanau: AEON Verlag & Studio) 217
- [2] Anguelova M D and Webster F 2006 *J. Geophys. Res.* **111**, C03017
- [3] Gasier P W *et al* 2004 *IEEE Trans. Geosci. Remote Sens.* **42** 2347
Bettenhausen M *et al* 2006 *IEEE Trans. Geosci. Remote Sens.* **44** 597
Anguelova M D and Gaiser P W 2013 *Rem. Sen. Environ.* **139** 8196
- [4] Anguelova M D *et al* 2010 *Proc. 17th Air-Sea Interaction Conf.* 174036
- [5] Salisbury D J *et al* 2013 *J. Geophys. Res.-Oceans* **118** 6201
Salisbury D J *et al* 2014 *Geophys. Res. Lett.* **41** 1616
- [6] Anguelova M D and Gaiser P W 2011 *J. Geophys Res.* **116** C11002
- [7] Mellville W K 1996, *Annu. Rev. Fluid Mech.* **28**, 279
Asher W *et al* 1998 *J. Mar. Tech. Soc.* **32** 32
- [8] Anguelova M D and Hwang P A 2012 *Proc. 18th Air-Sea Interaction Conf.* 209178
- [9] Phillips O M 1985 *J. Fluid Mech.* **156** 505
- [10] Anguelova M D and Hwang P A 2015, *J. Phys. Oceanogr.*, doi: 10.1175/JPO-D-15-0069.1
- [11] Fairall C W *et al* 1996 *J. Geophys. Res.*, **101** 3747
Fairall C W *et al* 2003 *J. Clim.* **16** 571
- [12] Fairall C W *et al* 2011 *J. Geophys. Res.* **116** C00F09
- [13] Woolf D K 1997 *Surface and Global Change* ed P S Liss and R A Duce (Cambridge, UK: Cambridge Univ. Press) 173
- [14] Edson J B *et al* 2011 *J. Geophys. Res.* **116** C00F10
- [15] Ho D T *et al* 2011 *J. Geophys. Res.* **116** C00F08
- [16] Monahan E C and O'Muircheartaigh I G 1980 *J. Phys. Oceanogr.* **10**, 2094
Ho D T *et al* 2006 *Geophys. Res. Lett.* **33** L16611
- [17] Andreas E L 2002, *Atmosphere-Ocean Interactions, Adv. Fluid Mech.* **33**, ed W Perrie (Boston: WIT) 1–46
- [18] Monahan E C *et al* 1986 *Oceanic Whitecaps and Their Role in Air-Sea Exchange Processes* ed E C Monahan and G Mac Niocaill (Dordrecht, The Netherlands: Reidel Publishing Company) 167–174
- [19] Andreas E L 1992 *J. Geophys. Res.* **97** 11429
- [20] Albert M F M A *et al* 2015 *Atmos. Chem. Phys. Discuss.* **15**, 21219
- [21] Jaeglé L *et al* 2011 *Atmos. Chem. Phys.* **11** 3137
- [22] Sofiev M *et al* 2011 *J. Geophys. Res.* **116** D21302
- [23] Norris S J *et al* 2008 *Atmos. Chem. Phys.* **8** 555
- [24] Grythe H *et al* 2014 *Atmos. Chem. Phys.* **14** 1277